Adaptive Speed Control for Permanent-Magnet Synchronous Motor System With Variations of Load Inertia

Shihua Li, *Member, IEEE*, and Zhigang Liu

***Abstract*—Considering the variations of inertia in real applications, an adaptive control scheme for the permanent-magnet synchronous motor speed-regulation system is proposed in this paper. First, a composite control method, i.e., the extended-state-observer (ESO)-based control method, is employed to ensure the performance of the closed-loop system. The ESO can estimate both the states and the disturbances simultaneously so that the composite speed controller can have a corresponding part to compensate for the disturbances. Then, considering the case of variations of load inertia, an adaptive control scheme is developed by analyzing the control performance relationship between the feedforward compensation gain and the system inertia. By using inertia identification techniques, a fuzzy-inferencer-based supervisor is designed to automatically tune the feedforward compensation gain according to the identified inertia. Simulation and experimental results both show that the proposed method achieves a better speed response in the presence of inertia variations.**

***Index Terms*—Adaptive control, extended state observer (ESO), fuzzy inferencer, inertia identification, permanent-magnet synchronous motor (PMSM), speed regulation.**

I. Introduction

PERMANENT-MAGNET synchronous motors (PMSM), which possess the characteristics of high power density, torque-to-inertia ratio, and efficiency, have been widely used in many industrial applications. It is well known that linear control schemes, e.g., the proportional–integral (PI) control scheme, are already widely applied in the PMSM system due to their relative simple implementation [37]. However, the PMSM servo system is a nonlinear system with unavoidable and unmeasured disturbances, as well as parameter variations [21]. This makes it very difficult for linear control algorithms to obtain a sufficiently high performance for this kind of nonlinear systems. It is reported that the PI control algorithm cannot assure a satisfying dynamic behavior in the entire operating range [12], [43].

Nonlinear control algorithms thus become a natural solution for controlling the PMSM. Recently, with the rapid progress in power electronics, microprocessors, especially digital signal processors (DSPs), and modern control theories, many researchers have aimed to develop nonlinear control methods for the PMSM, and various algorithms have been proposed, e.g., adaptive control [18], [31], [32], robust control [17], sliding-mode control [3], [42], input–output linearization control [12], backstepping control [41], [49], and intelligent control [26], [42], [43]. These algorithms have improved the control performance of PMSM from different aspects.

However, in real industrial applications, PMSM systems are always confronted with different disturbances. These disturbances may come internally, e.g., friction force and unmodeled dynamics, or externally, e.g., load disturbances. Conventional feedback-based control methods usually cannot react directly and fast to reject these disturbances, although these control methods can finally suppress them through feedback regulation in a relatively slow way. (The only exception is the sliding-mode control method, which shows a good robustness to disturbances. However, it faces an unavoidable application problem—chattering.) This results in a degradation of system performance when meeting severe disturbances.

One efficient way of improving system performance in such cases is to introduce a feedforward compensation part into the controller besides the conventional feedback part. Thus, a composite control method is obtained. Since, in real PMSM applications, it is usually impossible to measure the disturbances directly, disturbance estimation techniques have to be developed. The disturbance-observer (DOB)-based control method was originally presented by Ohnishi in 1987 [33]. Following this direction, many DOB-based control methods have been reported in different applications, e.g., robotic systems [5], hard disk drive systems [44], general motion control systems [7], [8], [27], [28], inverted-pendulum systems [19], missile systems [6], PMSM systems [20]–[22], other kinds of motor systems [40], and general control systems [2], [7], [8], [13], [23]. Among these results, different kinds of DOBs have been developed, including linear DOBs [20], [21], [23], [27], [40], [44], fuzzy DOBs [19], neural-network-based DOBs [22], other nonlinear DOBs [5]–[8], [13], [28], etc.

Another kind of disturbance estimation techniques is the extended state observer (ESO) [15], [16]. It regards the lumped disturbances of the system, which consists of internal dynamics and external disturbances, as a new state of the system. This observer is one order more than the usual state observer. It can estimate both the states and the lumped disturbances. Based on the ESO, a feedforward compensation for the disturbances can also be employed in the control design. A composite control

Manuscript received November 24, 2008; revised May 18, 2009. First published June 10, 2009; current version published July 24, 2009. This work was supported by the Natural Science Foundation of Jiangsu Province under Project BK2008295.

S. Li is with the School of Automation, Southeast University, Nanjing 210096, China (e-mail: lsh@seu.edu.cn).

Z. Liu is with Huawei Technologies Company, Ltd., Shenzhen 518129, China.

Digital Object Identifier 10.1109/TIE.2009.2024655

frame based on the ESO, called active disturbance rejection control or autodisturbance rejection control, is also developed. This method has also been applied in some industrial control problems, e.g., robotic systems [35], machining processes [45], manipulator systems [36], power converter [38], PMSM systems [29], [37], other motor systems [10], [34], and general control systems [39].

The ESO-based composite controller applied in the PMSM is robust to the disturbances to some extent [37]. However, in servo motor drive applications, variations of load inertia diminish the performance quality of the drives. In some applications, e.g., electric winding machine, the inertia of the whole system is time varying, which increases as time goes by. If the inertia of the system is increased to more than several times of the original inertia, the control performance cannot be guaranteed when the parameters of the controller are fixed [48]. High-performance drives generally require the identification of the moment of inertia of the whole system, including the motor and load. In [46], an inertia identification and an autotuning scheme of the control parameters for the position control of PMSM drives are presented. The control gains of the position control loop are tuned automatically corresponding to the inertia identified.

In this paper, combining the ESO with the inertia identification technique together, an adaptive controller for the PMSM speed-regulation system is developed to improve the adaptation of the closed-loop system to the variations of inertia. The two current loops still employ two standard PI controllers, and the speed loop employs an ESO-based composite controller. An ESO in the feedback path provides estimates of both the speed and the unknown lumped disturbances. The estimate of the lumped disturbances is employed for the feedforward compensation design of the control law such that the performance degradation caused by the disturbances can be suppressed. A torque DOB-based method is adopted to estimate the inertia of the PMSM and load, and then, the gain of feedforward compensation based on the ESO is autotuned according to the identified inertia. The effectiveness of this scheme is verified by both simulation and experimental results.

II. Problem Description

Taking the rotor coordinates ($d-q$ axes) of the motor as reference coordinates, the model of a surface-mounted PMSM motor can be described as [25]

$$\begin{pmatrix} \dot{i}_d \\ \dot{i}_q \\ \dot{\omega} \end{pmatrix} = \begin{pmatrix} -\frac{R}{L} & n_p\omega & 0 \\ -n_p\omega & -\frac{R}{L} & \frac{n_p\psi_f}{L} \\ 0 & -\frac{K_t}{J} & -\frac{B}{J} \end{pmatrix} \begin{pmatrix} i_d \\ i_q \\ \omega \end{pmatrix} + \begin{pmatrix} \frac{u_d}{L} \\ \frac{u_q}{L} \\ -\frac{T_L}{J} \end{pmatrix} \tag{1}$$

where

i_d, i_q	d- and q-axis stator currents, respectively;
u_d, u_q	d- and q-axis stator voltages, respectively;
n_p	number of pole pairs;
R	stator resistance;
L	stator inductance;
ψ_f	rotor flux linkage;
K_t	torque constant;
ω	angular velocity;
B	viscous friction coefficient;
J	moment of inertia;
T_L	load torque.

A well-known strategy to control a PMSM drive is the field-oriented vector control approach [4]. Under this scheme, the torque- and flux-producing components of the stator current are decoupled so that the independent torque and flux controls are possible as in dc motors. Also, a practical structure of cascade control loops, including a loop of speed and two loops of current, is employed. Usually, the d-axis reference current i_d^* is set to be $i_d^* = 0$ in order to approximately eliminate the couplings between angular velocity and currents. If the controllers for the two current loops work well, the output i_d satisfies $i_d \doteq i_d^* = 0$, and then, system (1) can be approximately reduced to the following form:

$$\begin{pmatrix} \dot{i}_q \\ \dot{\omega} \end{pmatrix} = \begin{pmatrix} -\frac{R}{L} & \frac{n_p\psi_f}{L} \\ -\frac{K_t}{J} & -\frac{B}{J} \end{pmatrix} \begin{pmatrix} i_q \\ \omega \end{pmatrix} + \begin{pmatrix} \frac{u_q}{L} \\ -\frac{T_L}{J} \end{pmatrix} \tag{2}$$

which makes the speed controller design simpler.

A schematic of the PMSM speed-regulation system based on vector control is shown in Fig. 1. As shown in Fig. 1, two PI algorithms are used in the two current loops, respectively. We mainly address the adaptive control design of the ESO-based composite control law for the speed loop such that the whole PMSM control system shows a good adaptation to the variations of load inertia.

III. Control Strategy

A. Speed Controller Design for PMSM

1) ESO-Based Controller for PMSM: The lumped disturbances of PMSM systems include internal disturbances, e.g., unmodeled dynamics and variations of parameters, and external disturbances, e.g., variations of load torque [15]. These disturbances will degrade the performance of the closed-loop system if we do not consider a corresponding feedforward compensation control design to suppress it. To do this, first, an estimate of the disturbances should be obtained. The ESO can be considered as a conventional state observer with one additional ability, i.e., disturbance estimation. It not only observes all the system states but also estimates the lumped disturbances.

Next, we design a composite speed-loop controller based on ESO techniques. The ESO-based control scheme for the PMSM is shown in Fig. 2. In Fig. 2, the "generalized PMSM" represents the two current loops that include the PMSM and other components, similar to that of Fig. 1. Note that a limit is imposed on the given current i_q^*. From the consideration of saturation, the absolute value of i_q^* should be limited to not exceed a given value $i_{q\max} > 0$. Thus, the relationship between i_q^* and u is

$$i_q^* = \mathrm{sat}(u) = \begin{cases} u, & |u| \le i_{q\max} \\ i_{q\max} \cdot \mathrm{sign}(u), & |u| > i_{q\max}. \end{cases}$$

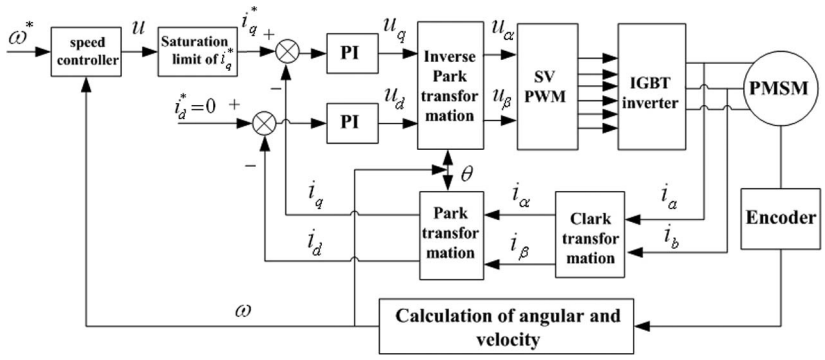

Fig. 1. Schematic diagram of the PMSM speed-regulation system based on vector control.

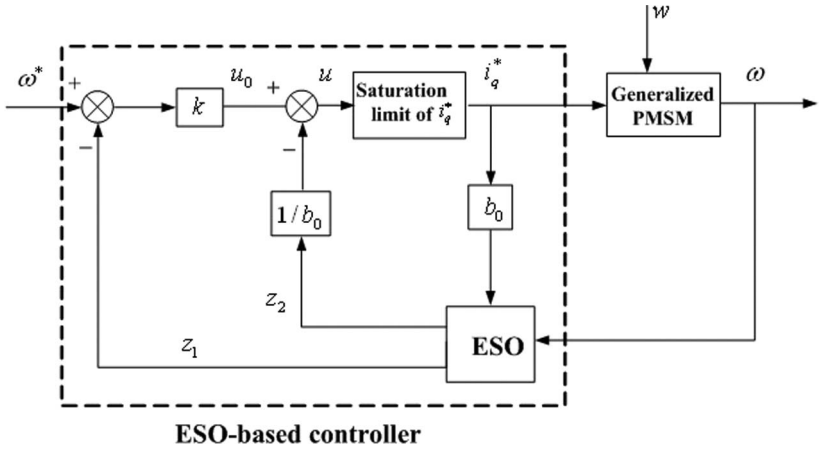

Fig. 2. Block diagram of the ESO-based controller for the PMSM system.

From (1), we can obtain

$$\dot{\omega} = \frac{K_t i_q}{J} - \frac{B\omega}{J} - \frac{T_L}{J} = a(t) + b_0 i_q^* \tag{3}$$

where $a(t) = -(B\omega/J) - (T_L/J) + (K_t/J)(i_q - i_q^*) + ((K_t/J) - b_0)i_q^*$ represents the lumped disturbances, including the friction, the external load disturbances, the tracking error of the current loop of i_q, and the modeling error. Note that b_0 is an estimate of K_t/J. Now, the control design of the speed loop is reduced to a first-order case.

Regarding $a(t)$ as an extended state, define

$$x_1 = \omega \quad x_2 = a(t).$$

Then, the dynamics of system (3) can be rearranged into the following state equation:

$$\dot{x}_1 = x_2 + b_0 i_q^* \quad \dot{x}_2 = c(t) \tag{4}$$

where $c(t) = \dot{a}(t)$. According to [30], a linear ESO can be constructed for (4) as follows:

$$\begin{aligned} \dot{z}_1 &= z_2 - 2p(z_1 - \omega) + b_0 i_q^* \\ \dot{z}_2 &= -p^2(z_1 - \omega) \end{aligned} \tag{5}$$

where $-p$ is the desired double pole of the ESO, with $p > 0$. Here, according to the analysis in [30], $z_1(t)$ is an estimate of the speed output ω, while $z_2(t)$ is an estimate of the lumped disturbances $a(t)$, i.e., $z_1(t) \to \omega(t)$ and $z_2(t) \to a(t)$. A composite control law for the speed loop is then designed as follows:

$$i_q^* = \text{sat}\left(u_0 - \frac{z_2}{b_0}\right), \qquad u_0 = k(\omega^* - z_1) \tag{6}$$

where k is the proportional gain, ω^* is the reference speed, and z_1 is an estimate of $\omega(t)$.

2) Performance Analysis: The ESO-based controller applied in the PMSM is robust to some extent. However, in most of the application circumstances, the PMSM drives different load devices that have different inertias. Variations of load inertia degrade the performance of the drives. If the inertia of the system is increased to more than several times of the original inertia, the control performance of the controller cannot be guaranteed when the parameters of the controller are fixed.

Next, we will show this phenomenon by simulation and experimental results, respectively. The specification of the PMSM is shown in Table I.

Here, in the simulation, the speed controller parameters of the speed loop are selected as $k = 0.012$ and $-p = -300$. At the initial stage, the motor inertia is assumed to be $J = J_n$, so b_0 is determined as $b_0 = K_t/J = K_t/J_n = 9033.7$. The PI parameters of both current loops are the same, the current-loop proportional gains are 50, and current-loop integral gains are 2500. The saturation limit of the q-axis reference current is ± 12 A.

TABLE I
SPECIFICATION OF THE PMSM

rated power P_N	0.75kw	rotor inertia J_n	$1.78{\cdot}10^{-4}\ kgm^2$
rated voltage U_N	103V	pole pairs n_p	4
rated current I_N	4.71A	stator resistance R	1.74Ω
rated speed n_N	3000r/min	torque constant K_t	1.608Nm/A
rated torque T_N	2.387Nm	viscous coefficient B	0.000074Nms/rad
stator inductance L	4mH		

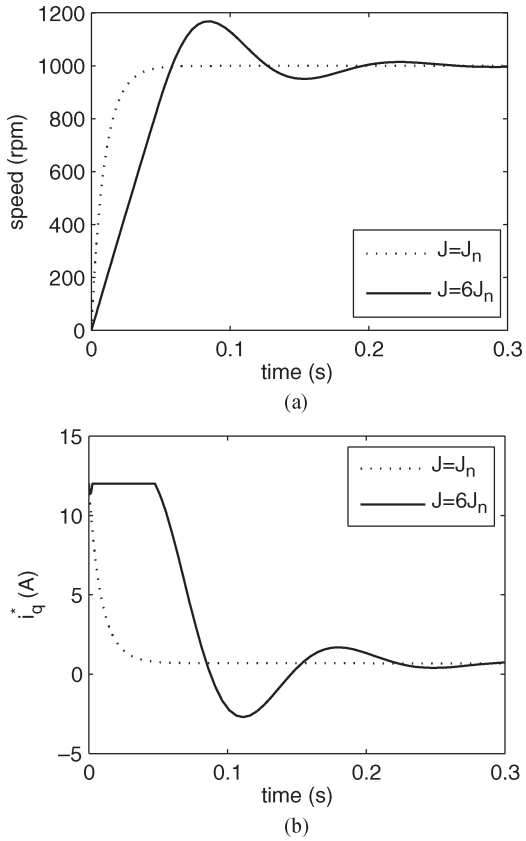

Fig. 3. Performance comparisons in the case of $J = J_n$ and $J = 6J_n$ (simulation). (a) Speed response. (b) i_q^* response.

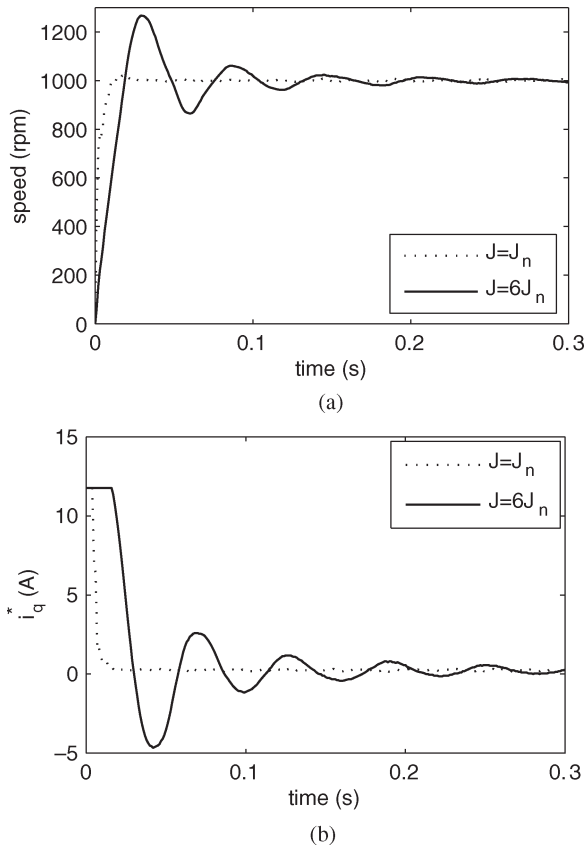

Fig. 4. Performance comparisons in the case of $J = J_n$ and $J = 6J_n$ (experiment). (a) Speed response. (b) i_q^* response.

The dashed lines in Fig. 3 show the response curves of speed and i_q^*, respectively, when the inertia of the system is J_n. The speed response has almost no overshoot and a short settling time (0.039 s) with 2% of the final value. The solid lines in Fig. 3 show the simulation results when the inertia of the system is increased to $6J_n$. From Fig. 3, we can see that the speed response has a bigger overshoot (16.83%) and a longer settling time (0.18 s) in the case of $J = 6J_n$ (solid line). The control performance of the speed controller becomes worse if the parameters of the speed controller are fixed when the inertia of the system is increased to $6J_n$. The reason is that the feedback compensation gain b_0 is still fixed to be K_t/J_n, while it is theoretically supposed to be tuned with the change of inertia, i.e., $b_0 = K_t/J$.

In the experiment, the parameters of the speed loop are selected as $k = 0.012$, $-p = -250$, and $b_0 = 8917$. The proportional gains of both current loops are selected to be 42, and both integral gains are 2600. The speed- and current-loop sampling periods are 250 and 60 μs, respectively. The saturation limit of the q-axis reference current is ± 11.78 A. The dashed lines in Fig. 4 show the response curves of speed and i_q^*, respectively, when the inertia of the system is J_n. The speed response has a small overshoot (2.2%) and a short settling time (0.01 s). When the inertia is increased to $6J_n$, the speed response (solid line) is shown in Fig. 4. The speed response also has a bigger overshoot (26.75%) and a longer settling time (0.147 s).

From the simulation and experimental results, we can see that the control performance of the closed-loop system will be diminished if the inertia of the whole system varies largely and the controller does not have any adaptation ability to handle this kind of changes. In order to get a higher performance drive, the inertia of the system should be identified, and an adaptive speed controller should be developed.

3) Discussion: For simplicity, in the following analysis, we do not consider the effect of saturation, letting the output of the speed-loop controller $i_q^* = u$.

From (3) and (6), we can obtain

$$\dot{\omega} = a(t) + b_0 i_q^* = a(t) + b_0 \left(u_0 - \frac{z_2}{b_0}\right) = (a(t) - z_2) + b_0 u_0 \quad (7)$$

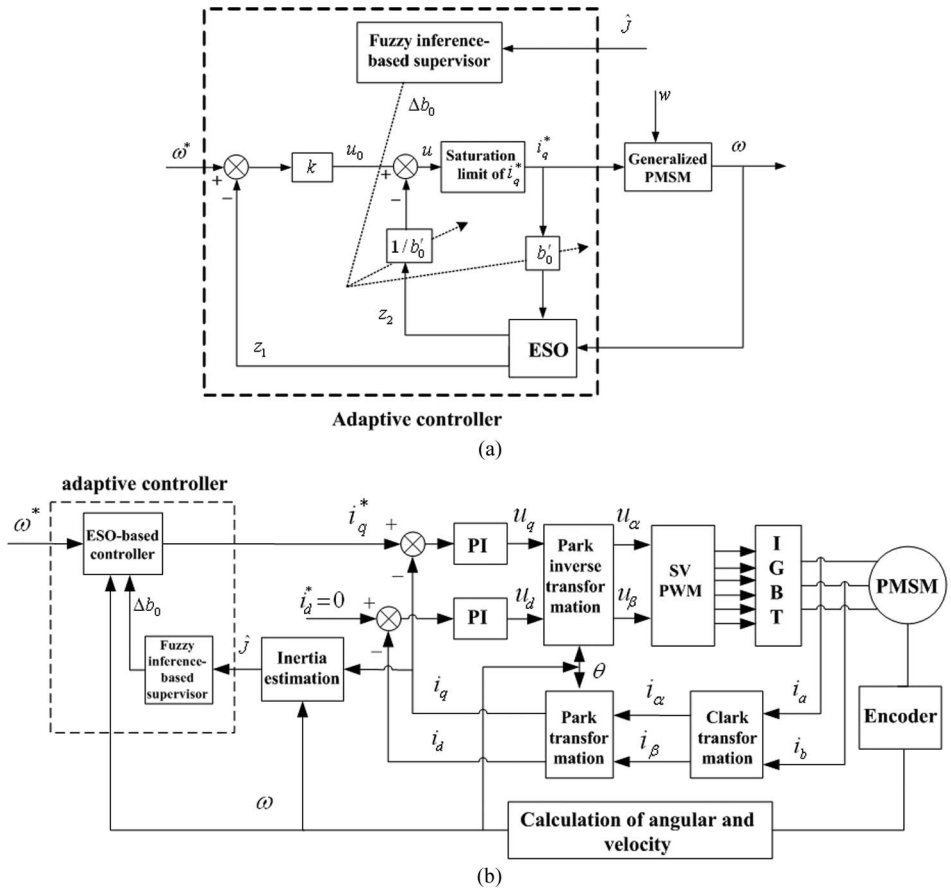

Fig. 5. Adaptive control scheme for the PMSM speed-regulation system. (a) Detail diagram of the adaptive controller. (b) Whole schematic diagram.

where z_2 is an estimate of $a(t)$ and b_0 is an estimate of $b = K_t/J$.

Note that the double pole $-p > 0$ of the ESO can be tuned to be large enough to ensure the observation precision of z_2 to $a(t)$. Thus, if z_2 is a good estimation of $a(t)$, i.e., $z_2 \to a(t)$, then (7) can approximately be reduced to

$$\dot{\omega} = (a(t) - z_2) + b_0 u_0 \doteq b_0 u_0. \tag{8}$$

When the inertia of the system is increased, b becomes smaller, and b_0 (an estimate of b) should become smaller with b. However, in practical applications, b_0 is usually fixed to be a constant $b_0 = K_t/J_n$, which is not changed with the inertia. Therefore, when the inertia of the system is increased, if neither the control term u_0 nor b_0 changes, the term $b_0 u_0$ becomes bigger and makes $\dot{\omega}$ become bigger according to (8). Therefore, the speed response has a bigger overshoot and a longer settling time. To get a better speed response, the $b_0 u_0$ term should correspondingly be decreased, i.e., b_0 should be reduced when the inertia of the system is increased since b_0 is an estimate of K_t/J.

B. Adaptive Controller Design of PMSM

Thus, the tuning strategy is to tune b_0. If we can obtain the inertia of the PMSM, the parameter b_0 can automatically be tuned. Therefore, an adaptive controller is presented to automatically tune b_0 according to the estimated inertia.

The design of the adaptive controller is as follows.

1) ESO

$$\begin{aligned} \dot{z}_1 &= z_2 - 2p(z_1 - \omega) + \acute{b}_0 i_q^* \\ \dot{z}_2 &= -p^2(z_1 - \omega) \end{aligned} \tag{9}$$

where z_1 is an estimate of angular velocity ω and z_2 is an estimate of system disturbances $a(t)$.

2) Control law

$$i_q^* = \text{sat}\left(u_0 - \frac{z_2}{\acute{b}_0}\right), \qquad u_0 = k(\omega^* - z_1) \tag{10}$$

where k is the proportional gain and ω^* is the reference speed, and $\acute{b}_0$ can be tuned according to the identified inertia.

The block diagram of the adaptive speed controller for the PMSM is shown in Fig. 5(a). A parameter autotuning strategy is adopted to tune the parameter $\acute{b}_0$ by using the estimated inertia $\hat{J}$. Thus, the adaptive control scheme of the PMSM speed-regulation system is shown in Fig. 5(b).

C. Inertia Identification

The methods of inertia identification for PMSM drives can be divided into three categories. One method is based on speed response. In [48], a method using the saturation limits of current is presented, which uses motor speed response to

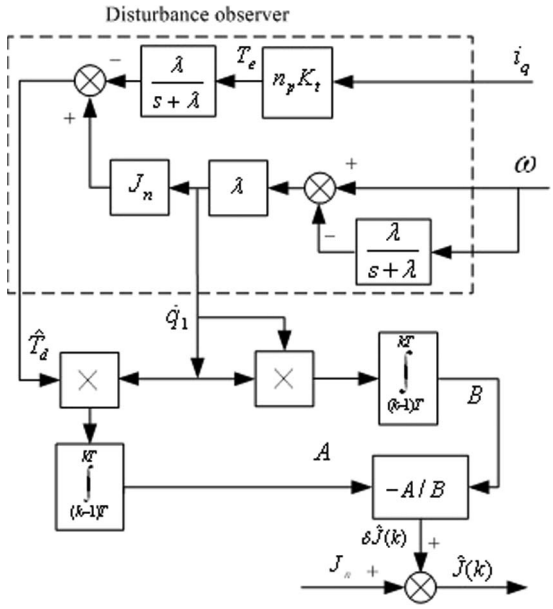

Fig. 6. Block diagram of inertia estimation.

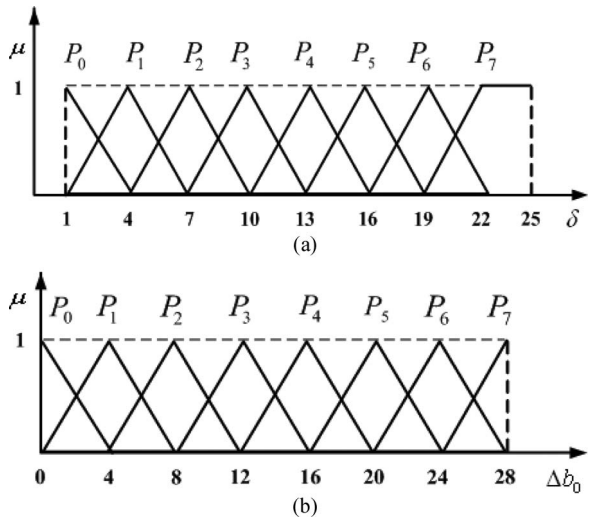

Fig. 7. Membership functions. (a) Membership function of inertia ratio δ. (b) Membership function of Δb_0.

calculate inertia through changing the saturation limits of current. The second method is to use a model reference adaptive method. In [11] and [14], model reference adaptive methods are implemented to identify drive inertia. However, both of the aforementioned methods do not consider the effect of viscous friction in the model. The third method is based on DOB to identify inertia. This method uses disturbance estimators to estimate the external disturbances and friction in the model and then obtain an estimate of inertia [1], [9], [46]. In [1], a DOB is used for inertia identification. Inertia is obtained by using the orthogonal relation among the estimated torque components, which include the inertia variation torque, the viscous torque, and the constant disturbance torque.

In this paper, we adopt the third method, i.e., the DOB-based method, to identify inertia. The detailed process of inertia identification can be found in [1]. Furthermore, the method can identify inertia online. The effectiveness of the method is verified by experimental results.

The estimation equation of inertia is as follows [1]:

$$\delta J(k) = -\lim_{k\longrightarrow\infty} \frac{\int_{(k-1)T}^{kT} \hat{T}_d(t) \times \dot{q}_1(t)dt}{\int_{(k-1)T}^{kT} \dot{q}_1^2(t)dt} \tag{11}$$

$$\hat{J}(k) = J_n + \delta J(k) \tag{12}$$

where δJ is the estimated inertia variation during the kth sampling period kT, $\hat{J}(k)$ is the estimated value of inertia, $\hat{T}_d(t)$ is the estimated disturbance torque, and $q_1(t)$ is the state variable.

In this method, a test signal for inertia identification is the periodic speed command that satisfies

$$\omega^*(t+T) = \omega^*(t)$$

where T is the period of speed command.

Fig. 6 is the block diagram of the inertia estimation [1].

D. Fuzzy Implementation of Adaptive Compensation

After the estimation of inertia, we can tune the parameter $\acute{b}_0$ of the speed controller when inertia varies, although $\acute{b}_0$ is theoretically supposed to be tuned with the change of inertia, i.e., $\acute{b}_0 = K_t/J$. However, in practical applications, in the cases of inertia variations, we cannot really take $\acute{b}_0 = K_t/J$ since the control saturation has to be considered. To ensure the performance of this adaptive control scheme, a practical performance relationship between $\acute{b}_0$ and inertia J should be obtained. Some expert knowledge from simulation and experimental results needs to be employed to help us decide the tuning expression for the feedforward compensation gain $\acute{b}_0$. Usually, it is not easy to express this knowledge by a precise mathematical model. Also, here, the parameter $\acute{b}_0$ does not need to be sensitive to the variations of inertia.

Therefore, a fuzzy inferencer [24], [47] is suitable and adopted to describe the autotuning function for the parameter $\acute{b}_0$. In addition, its implementation is simple and straightforward. The fuzzy implementation is about the one-input–one-output case. By simulation and experiment tests, we finally obtain the available groups of membership functions and fuzzy rules, which will subsequently be introduced.

When the inertia of the system is estimated, the ratio of the actual inertia to the original inertia $\delta = \hat{J}/J_n$ can be obtained. The inertia ratio δ is used as the input of the fuzzy inferencer, while the change of $\acute{b}_0$, i.e., Δb_0, is utilized as the output of the fuzzy inferencer. The final parameter after fuzzy tuning can be expressed as follows:

$$\acute{b}_0 = b_0 - a\Delta b_0, \qquad a, \Delta b_0 > 0 \tag{13}$$

where a is the proportional factor.

Here, assume that the ratio of inertia $\delta = \hat{J}/J_n$ satisfies $\delta \leq 25$. Then, the fuzzy set of δ can be chosen as P_0, P_1, P_2, P_3, P_4, P_5, P_6, P_7. The fuzzy set of Δb_0 can also be chosen as P_0, P_1, P_2, P_3, P_4, P_5, P_6, P_7. The membership functions of the two fuzzy sets are shown in Fig. 7. The fuzzy inference rules are as follows: If δ is P_i, then Δb_0 is P_i $(i = 0, 1, 2, \ldots, 7)$.

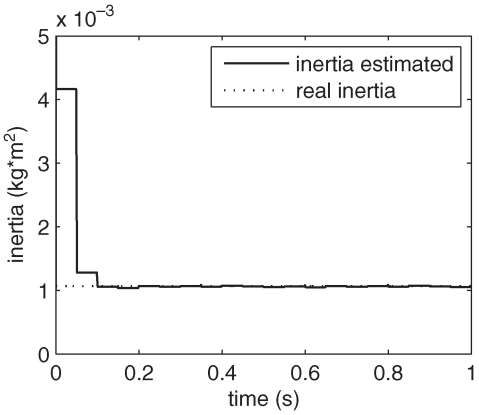

Fig. 8. Identification of (solid line) inertia and (dashed line) real inertia (simulation).

Note that the selection of the value domain of Δb_0 is not unique. Here, in Fig. 7(b), Δb_0 is taken to satisfy $0 < \Delta b_0 \leq 28$ in accordance with that of the following simulation and experiment.

In this paper, a Mamdani-type fuzzy inferencer is adopted, and the center-of-gravity method is used for defuzzification to obtain Δb_0. Using (13), we can obtain the parameter $\acute{b}_0$ after fuzzy inference.

Remark 1: It should be pointed out that a nonlinear ESO can also be used to estimate the disturbances [15]. The advantages of nonlinear ESO are that it may obtain a better observation precision and a faster converging estimation. However, it needs to tune more parameters to ensure the estimation performance. Since the main purpose of this paper is to build an effective parameter tuning mechanism for the ESO-based composite controller to follow the variations of inertia, for simplicity, we only consider the linear ESO-based scheme. It can be observed from the previous analysis that the adaptive control scheme here can also be generalized to the case of nonlinear ESO.

IV. Simulation and Experimental Results

A. Simulation Results

The specification of the PMSM is the same as that in Table I, and other parameters of the simulation in this paper are the same as that in Section III-A2. For the DOB employed for the identification of inertia, the pole $-\lambda$ in Fig. 6 is selected as $-\lambda = -200$. To test the inertia, the speed command signal is chosen as $\omega^* = 300 + 100\sin(40\pi t)$. For the fuzzy inferencer, the membership functions of input and output, and the inference rules are the same as that in Section III-D. The proportional factor a is selected as 318.5.

Fig. 8 is the simulation result of inertia identification when the inertia of the system is increased to $6J_n$. The dashed line is the real inertia. We can see that the method of inertia identification (solid line) has a good estimation effect.

After inertia identification, the ratio of inertia δ is obtained, i.e., $\delta = 6$. According to the fuzzy rule and fuzzy inference, the output of the fuzzy inferencer is $\Delta b_0 = 6.5$. Note that, as before, $b_0 = 9033.7$. Thus, $\acute{b}_0 = b_0 - a\Delta b_0 = 6963.5$. The speed response before and after parameter autotuning is shown in Fig. 9.

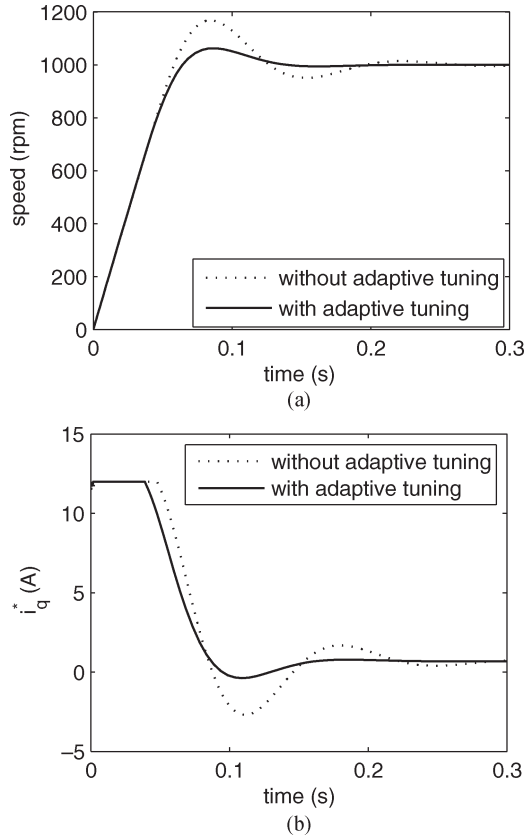

Fig. 9. Performance comparisons under the adaptive control law (10) and nonadaptive control law (6). (a) Speed response. (b) i_q^* response.

Compared with the speed response without adaptive tuning (16.83% overshoot and 0.18-s settling time), the speed response under adaptive parameter tuning has a much smaller overshoot (6.3%) and a shorter settling time (0.12 s). After the system inertia varies, the parameter $\acute{b}_0$ is tuned according to the inertia, and then, the ESO can track the disturbances with a better response, and the compensation term $z_2/\acute{b}_0$ has a better feedforward compensation effect. Therefore, the PMSM speed-regulation system has a better speed-adjusting performance.

B. Experimental Results

To evaluate the performance of the proposed method, the experimental setup system for the speed control of a PMSM has been built. Its configuration and the experimental test setup are shown in Figs. 10 and 11, respectively. The whole speed control algorithms, including the space-vector pulsewidth modulation technique, are implemented by the program of the DSP TMS320F2808 with a clock frequency of 100 MHz. The control algorithm is implemented using a C-program. The speed- and current-loop sampling periods are 250 and 60 μs, respectively. The saturation limit of the q-axis reference current is ± 11.78 A. The PMSM is driven by a three-phase PWM inverter with an intelligent power module with a switching frequency of 10 kHz. The phase currents are measured by Hall-effect devices and are converted through two 12-b A/D

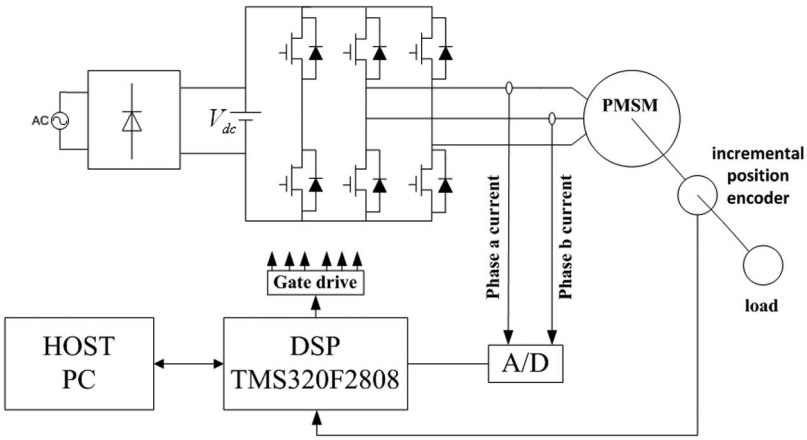

Fig. 10. Configuration of the experimental system.

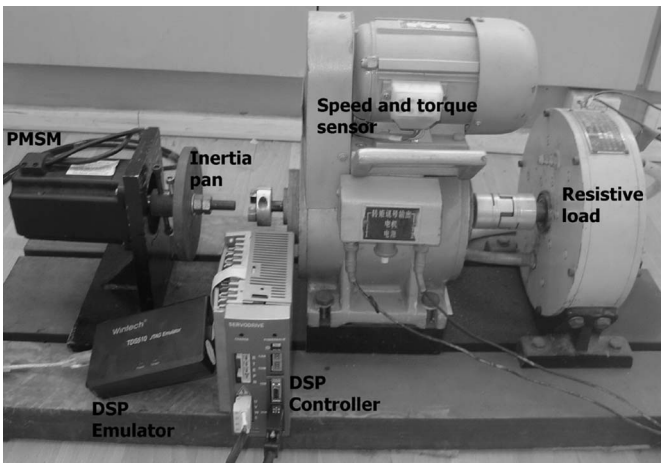

Fig. 11. Experimental test setup.

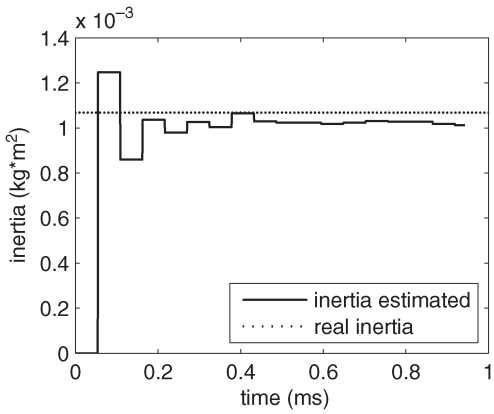

Fig. 12. Identification of (solid line) inertia and (dashed line) real inertia (experiment).

converters. An incremental position encoder of 2500 lines is used to measure the rotor speed and absolute rotor position.

The specification of the PMSM is the same as that in Table I, and other parameters of the experiments in this paper are the same as that in Section III-A2. The pole of the DOB employed for identifying inertia is selected as $-\lambda = -200$. To test the inertia, the speed command signal is chosen as $\omega^* = 500 + 90\sin(4.5\pi t)$. Different specially designed mechanical inertia pans can be selected to attach to the motor so that the inertia of the whole system is increased to different times of J_n. In this experiment, four kinds of inertia pans, which are about 5, 10, 15, and 20 times of J_n, respectively, are used for helping one decide the fuzzy tuning implementation for the feedforward compensation gain $\acute{b}_0$ and verifying the performance of the proposed adaptive control scheme.

Fig. 12 shows the experimental result of inertia identification when the inertia of the system is increased to $6J_n$. Note that a small estimation error between the estimated inertia and the real inertia has little influence on the final control effect since our adaptive control scheme does not need to be sensitive to the variations of inertia.

After inertia identification, the ratio of inertia δ is obtained, i.e., $\delta = 6$. According to the fuzzy rule and fuzzy inference, the output of the fuzzy inferencer is $\Delta b_0 = 6.5$. Note that, in the experiment, b_0 is taken to be $b_0 = 8917$, which is a little different with that of the simulation. The proportional factor is still $a = 318.5$. It can be obtained that $\acute{b}_0 = b_0 - a\Delta b_0 = 6782$. Fig. 13 shows the speed and i_q^* response curves. From Fig. 13, it can be seen that the closed-loop system has a better speed response after the feedforward compensation gain $\acute{b}_0$ is fuzzy-tuned according to the estimated inertia. Compared with the speed response without adaptive tuning (26.75% overshoot and 0.147-s settling time), the speed response under adaptive parameter tuning has a much smaller overshoot (2.65%) and a shorter settling time (0.042 s).

From these simulation and experimental results, it can be concluded that the speed controller with parameter autotuning possesses a good adaptation and a much better dynamic performance against inertia variations.

V. Conclusion

A PMSM may face the application cases of variations of load inertia if the controller does not have an adaptive mechanism to tune the control parameter according to the varying inertia. The performance of the closed-loop system will be diminished. To this end, in this paper, an adaptive control scheme for the PMSM speed-regulation system has been proposed. An ESO-based composite control method has been employed to

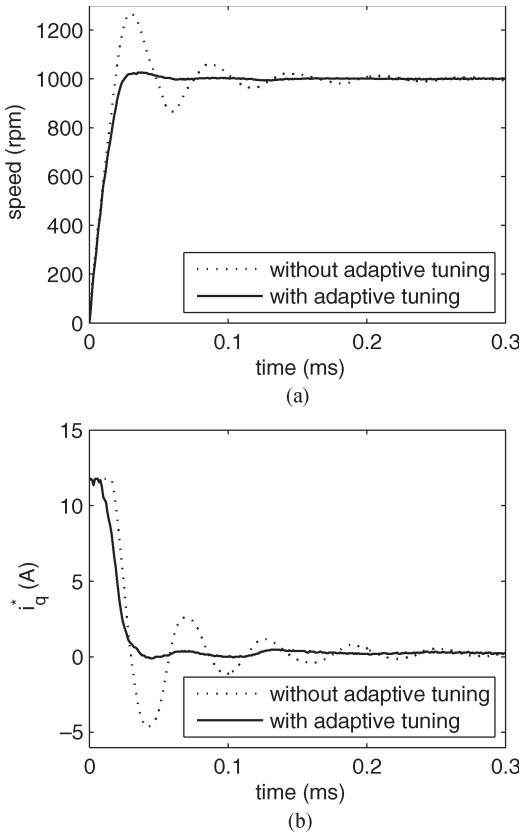

Fig. 13. Performance comparisons under the adaptive control law (10) and nonadaptive control law (6). (a) Speed response. (b) Speed-loop controller output response.

ensure the performance of the closed-loop system. The ESO can estimate not only the states but also the disturbances simultaneously so that the composite speed controller can have a corresponding part to compensate for the disturbances. Then, considering the case of variations of load inertia, an adaptive control scheme has been developed by analyzing the control performance relationship between the feedforward compensation gain and the system inertia. By using inertia identification techniques, a fuzzy-inferencer-based supervisor has been designed to automatically tune the feedforward compensation gain according to the identified inertia. Both simulation and experimental results have shown that the proposed method achieves a better speed response in the presence of inertia variations.

REFERENCES

[1] I. Awaya, Y. Kato, I. Miyake, and M. Ito, "New motion control with inertia identification function using disturbance observer," in *Proc. Power Electron. Motion Control Conf.*, 1992, pp. 77–81.

[2] J. Back and H. Shim, "Adding robustness to nominal output-feedback controllers for uncertain nonlinear systems: A nonlinear version of disturbance observer," *Automatica*, vol. 44, no. 10, pp. 2528–2537, Oct. 2008.

[3] I. C. Baik, K.-H. Kim, and M. J. Youn, "Robust nonlinear speed control of PM synchronous motor using boundary layer integral sliding mode control technique," *IEEE Trans. Control Syst. Technol.*, vol. 8, no. 1, pp. 47–54, Jan. 2000.

[4] F. Blaschke, "The principle of field orientation as applied to the new transvector closed loop control for rotating machine," *Siemens Rev.*, vol. 39, no. 5, pp. 217–220, 1972.

[5] W.-H. Chen, D. J. Ballance, P. J. Gawthrop, J. J. Gribble, and J. O'Reilly, "Nonlinear disturbance observer for two-link robotic manipulators," *IEEE Trans. Ind. Electron.*, vol. 47, no. 4, pp. 932–938, Aug. 2000.

[6] W.-H. Chen, "Nonlinear disturbance observer enhanced dynamic inversion control of missiles," *J. Guid. Control Dyn.*, vol. 26, no. 1, pp. 161–166, Jan./Feb. 2003.

[7] W.-H. Chen, "Disturbance observer based control for nonlinear systems," *IEEE/ASME Trans. Mechatronics*, vol. 9, no. 4, pp. 706–710, Dec. 2004.

[8] X. Chen, S. Komada, and T. Fukuda, "Design of a nonlinear disturbance observer," *IEEE Trans. Ind. Electron.*, vol. 47, no. 2, pp. 429–437, Apr. 2000.

[9] J. W. Choi, S. C. Lee, and H. G. Kim, "Inertia identification algorithm for high-performance speed control of electric motors," *Proc. Inst. Elect. Eng.—Electr. Power Appl.*, vol. 153, no. 3, pp. 379–386, May 2006.

[10] G. Feng, L. Huang, and Y.-F. Liu, "A new robust algorithm to improve the dynamic performance on the speed control of induction motor drive," *IEEE Trans. Power Electron.*, vol. 19, no. 6, pp. 1614–1627, Nov. 2004.

[11] K. Fujita and K. Sado, "Instantaneous speed detection with parameter identification for AC servo system," *IEEE Trans. Ind. Appl.*, vol. 28, no. 4, pp. 864–872, Jul./Aug. 1992.

[12] B. Grcar, P. Cafuta, M. Znidaric, and F. Gausch, "Nonlinear control of synchronous servo drive," *IEEE Trans. Control Syst. Technol.*, vol. 4, no. 2, pp. 177–184, Mar. 1996.

[13] L. Guo and W. H. Chen, "Disturbance attenuation and rejection for a class of nonlinear systems via DOBC approach," *Int. J. Robust Nonlinear Control*, vol. 15, no. 3, pp. 109–125, Feb. 2005.

[14] Y. J. Guo, L. P. Huang, Y. Qiu, and M. Muramatsu, "Inertia identification and auto-tuning of Induction motor using MARS," in *Proc. Power Electron. Motion Control Conf.*, 2000, pp. 1006–1011.

[15] J. Q. Han, "The extended state observer of a class of uncertain systems," *Control Decision*, vol. 10, no. 1, pp. 85–88, 1995, (in Chinese).

[16] J. Q. Han, "From PID to active disturbance rejection control," *IEEE Trans. Ind. Electron.*, vol. 56, no. 3, pp. 900–906, Mar. 2009.

[17] T.-L. Hsien, Y.-Y. Sun, and M.-C. Tsai, "H_∞ control for a sensorless permanent-magnet synchronous drive," *Proc. Inst. Elect. Eng.—Electr. Power Appl.*, vol. 144, no. 3, pp. 173–181, May 1997.

[18] H. Z. Jin and J. M. Lee, "An RMRAC current regulator for permanent-magnet synchronous motor based on statistical model interpretation," *IEEE Trans. Ind. Electron.*, vol. 56, no. 1, pp. 169–177, Jan. 2009.

[19] E. Kim, "A fuzzy disturbance observer and its application to control," *IEEE Trans. Fuzzy Syst.*, vol. 10, no. 1, pp. 77–84, Feb. 2002.

[20] K. H. Kim, I. C. Baik, G.-W. Moon, and M.-J. Youn, "A current control for a permanent magnet synchronous motor with a simple disturbance estimation scheme," *IEEE Trans. Control Syst. Technol.*, vol. 7, no. 5, pp. 630–633, Sep. 1999.

[21] K. H. Kim and M.-J. Youn, "A nonlinear speed control for a PM synchronous motor using a simple disturbance estimation technique," *IEEE Trans. Ind. Electron.*, vol. 49, no. 3, pp. 524–535, Jun. 2002.

[22] J.-S. Ko and B.-M. Han, "Precision position control of PMSM using neural network disturbance observer on forced nominal plant," in *Proc. IEEE Int. Conf. Mechatronics*, 2006, pp. 316–320.

[23] H. Kobayashi, S. Katsura, and K. Ohnishi, "An analysis of parameter variations of disturbance observer for motion control," *IEEE Trans. Ind. Electron.*, vol. 54, no. 6, pp. 3413–3421, Dec. 2007.

[24] B. Kosko, *NN and Fuzzy System: A Dynamical Systems Approach to Machine Intelligence*. Englewood Cliffs, NJ: Prentice-Hall, 1992.

[25] P. C. Krause, *Analysis of Electric Machinery*, 2nd ed. New York: McGraw-Hill, 1995.

[26] Y.-S. Kung and M.-H. Tsai, "FPGA-based speed control IC for PMSM drive with adaptive fuzzy control," *IEEE Trans. Power Electron.*, vol. 22, no. 6, pp. 2476–2486, Nov. 2007.

[27] H. S. Lee and M. Tomizuka, "Robust motion controller design for high-accuracy positioning systems," *IEEE Trans. Ind. Electron.*, vol. 43, no. 1, pp. 48–55, Feb. 1996.

[28] F.-J. Lin, P.-H. Chou, and Y.-S. Kung, "Robust fuzzy neural network controller with nonlinear disturbance observer for two-axis motion control system," *IET Control Theory Appl.*, vol. 2, no. 2, pp. 151–167, Feb. 2008.

[29] Z. G. Liu and S. H. Li, "Active disturbance rejection controller based on PMSM model identification and compensation," *Proc. Chin. Soc. Elect. Eng.*, vol. 28, no. 24, pp. 118–123, 2008, (in Chinese).

[30] R. Miklosovic and Z. Q. Gao, "A robust two-degree-of-freedom control design technique and its practical application," in *Conf. Rec. 39th IEEE IAS Annu. Meeting*, 2004, pp. 1495–1502.

[31] Y. A.-R. I. Mohamed, "Design and implementation of a robust current-control scheme for a PMSM vector drive with a simple adaptive disturbance observer," *IEEE Trans. Ind. Electron.*, vol. 54, no. 4, pp. 1981–1988, Aug. 2007.

[32] Y. A.-R. I. Mohamed and E. F. El-Saadany, "A current control scheme with an adaptive internal model for torque ripple minimization and robust current regulation in PMSM drive systems," *IEEE Trans. Energy Convers.*, vol. 23, no. 1, pp. 92–100, Mar. 2008.
[33] K. Ohnishi, "A new servo method in mechatronics," *Trans. Jpn. Soc. Elect. Eng.*, vol. 107-D, pp. 83–86, 1987.
[34] J. F. Pan, N. C. Cheung, and J. M. Yang, "Auto-disturbance rejection controller for novel planar switched reluctance motor," *Proc. Inst. Elect. Eng.—Electr. Power Appl.*, vol. 153, no. 2, pp. 307–316, Mar. 2006.
[35] J. Su, W. Qiu, H. Ma, and P.-Y. Woo, "Calibration-free robotic eye-hand coordination based on an auto disturbance-rejection controller," *IEEE Trans. Robot.*, vol. 20, no. 5, pp. 899–907, Oct. 2004.
[36] Y. X. Su, B. Y. Duan, C. H. Zheng, Y. F. Zhang, G. D. Chen, and J. W. Mi, "Disturbance-rejection high-precision motion control of a Stewart platform," *IEEE Trans. Control Syst. Technol.*, vol. 12, no. 3, pp. 364–374, May 2004.
[37] Y. X. Su, C. H. Zheng, and B. Y. Duan, "Automatic disturbances rejection controller for precise motion control of permanent-magnet synchronous motors," *IEEE Trans. Ind. Electron.*, vol. 52, no. 3, pp. 814–823, Jun. 2005.
[38] B. Sun and Z. Gao, "A DSP-based active disturbance rejection control design for a 1-kW H-bridge DC–DC power converter," *IEEE Trans. Ind. Electron.*, vol. 52, no. 5, pp. 1271–1277, Oct. 2005.
[39] D. Sun, "Comments on active disturbance rejection control," *IEEE Trans. Ind. Electron.*, vol. 54, no. 6, pp. 3428–3429, Dec. 2007.
[40] T. Umeno and Y. Hori, "Robust speed control of DC servomotors using modern two degrees-of-freedom controller design," *IEEE Trans. Ind. Electron.*, vol. 38, no. 5, pp. 363–368, Oct. 1991.
[41] D. M. Vilathgamuwa, M. A. Rahman, K. Tseng, and M. N. Uddin, "Nonlinear control of interior permanent magnet synchronous motor," *IEEE Trans. Ind. Appl.*, vol. 39, no. 2, pp. 408–416, Mar./Apr. 2003.
[42] R. J. Wai, "Total sliding-mode controller for PM synchronous servo motor drive using recurrent fuzzy neural network," *IEEE Trans. Ind. Electron.*, vol. 48, no. 5, pp. 926–944, Oct. 2001.
[43] G. J. Wang, C. T. Fong, and K. J. Chang, "Neural-network-based self tuning PI controller for precise motion control of PMAC motors," *IEEE Trans. Ind. Electron.*, vol. 48, no. 2, pp. 408–415, Apr. 2001.
[44] M. T. White, M. Tomizuka, and C. Smith, "Improved track following in magnetic disk drives using a disturbance observer," *IEEE/ASME Trans. Mechatronics*, vol. 5, no. 1, pp. 3–11, Mar. 2000.
[45] D. Wu, K. Chen, and X. Wang, "Tracking control and active disturbance rejection with application to noncircular machining," *Int. J. Mach. Tools Manufacture*, vol. 47, no. 15, pp. 2207–2217, Dec. 2007.
[46] S. M. Yang and Y. J. Deng, "Observer-based inertia identification for autotuning servo motor drives," in *Conf. Rec. 40th IEEE IAS Annu. Meeting*, 2005, pp. 968–972.
[47] L. Zadeh, "Outline of a new approach to the analysis of complex systems and decision processes," *IEEE Trans. Syst., Man, Cybern.*, vol. SMC-3, no. 1, pp. 28–44, Jan. 1973.
[48] B. Zhang, Y. Li, and Y. S. Zuo, "A DSP-based fully digital PMSM servo driving using on-line self-tuning PI controller," in *Proc. 3rd Power Electron. Motion Control Conf.*, 2000, pp. 1012–1017.
[49] J. Zhou and Y. Wang, "Adaptive backstepping speed controller design for a permanent magnet synchronous motor," *Proc. Inst. Elect. Eng.—Electr. Power Appl.*, vol. 149, no. 2, pp. 165–172, Mar. 2002.

Shihua Li (M'05) was born in Pingxiang, China, in 1975. He received the B.S., M.S., and Ph.D. degrees in automatic control from Southeast University, Nanjing, China, in 1995, 1998, and 2001, respectively.

Since 2001, he has been with the School of Automation, Southeast University, where he is currently a Professor. His main research interests include nonlinear control theory with applications to robot, spacecraft, ac motor, and other mechanical systems.

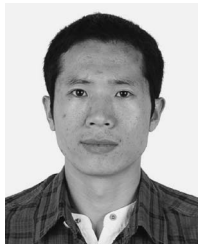

Zhigang Liu was born in Fugou, China, in 1982. He received the B.S. degree in automatic control from Hohai University, Nanjing, China, in 2005, and the M.S. degree in automatic control from Southeast University, Nanjing, in 2008.

He is currently with Huawei Technologies Company, Ltd., Shenzhen, China.